

Electronic structure, vibrational stability, infra-red, and Raman spectra of $B_{24}N_{24}$ cages

Rajendra R. Zope^{a,*} Tunna Baruah^{b,c} Mark R. Pederson^c
Brett I. Dunlap^d

^a*Department of Chemistry, George Washington University, Washington DC, 20052, USA*

^b*Department of Physics, Georgetown University, Washington DC, 20057, USA*

^c*Center for Computational Materials Science, US Naval Research Laboratory, Washington DC 20375, USA*

^d*Code 6189, Theoretical Chemistry Section, US Naval Research Laboratory, Washington, DC 20375, USA*

Abstract

We examine the vibrational stability of three candidate structures for the $B_{24}N_{24}$ cage and report their infra-red (IR) and Raman spectra. The candidate structures considered are a round cage with octahedral O_h symmetry, a cage with S_4 symmetry that satisfies the isolated square rule, and a cage of S_8 symmetry, which combines the caps of the (4,4) nanotube, and contains two extra squares and octagons. The calculations are performed within density functional theory, at the all electron level, with large basis sets, and within the generalized gradient approximation. The vertical ionization potential (VIP) and static dipole polarizability are also reported. The S_4 and S_8 cages are energetically nearly degenerate and are favored over the O_h cage which has six extra octagons and squares. The IR and Raman spectra of the three clusters show notable differences providing thereby a way to identify and possibly synthesize the cages.

Key words: boron nitride, nanotubes, cages, fullerene, infra-red, ionization potential and polarizability

PACS: 36.40.-c, 73.22.-f, 61.48.+c

* Fax: +1-202-767-1716

Email addresses: rzope@alchemy.nrl.navy.mil (Rajendra R. Zope),
baruah@dave.nrl.navy.mil (Tunna Baruah), pederson@dave.nrl.navy.mil
(Mark R. Pederson), dunlap@nrl.navy.mil (Brett I. Dunlap).

Recently, boron nitride (BN) cages were synthesized and detected by laser desorption time of flight mass spectroscopy [1]. The $B_{24}N_{24}$ cluster was observed in abundance and its structure was proposed to be a round cage structure with octahedral (\emptyset) symmetry (Cf. Fig. 1), in an analogy to the icosahedral C_{60} cluster. It consists of alternate BN atoms and is made round by introducing eighteen defects: six octagons and twelve squares, in the hexagonal network of a single BN sheet. In the icosahedral C_{60} fullerene every carbon atom is equivalent by symmetry. Similarly every boron or nitrogen atom in this octahedral structure is equivalent by symmetry. Taking a cue from the similarity of C_{60} fullerene and the O $B_{24}N_{24}$ cage it was suggested that the two halves of the round octahedral cage can form hemispherical caps for the (4,4) BN nanotubes [2] analogous to C_{60} hemispheres capping the (5,5) carbon nanotube [3]. Further by Euler theorem, in analogy to the twelve isolated pentagons of C_{60} , six isolated squares close the alternate BN fullerenes [4,5]. For the $B_{24}N_{24}$, the resultant cage (Cf. Fig. 1) has S_4 symmetry [5]. In a recent study [6] that examined seven candidate structures for the $B_{24}N_{24}$ geometry, the S_4 cage was found to be energetically favorable over the \emptyset cage in agreement with our work. A new, most stable cage structure was found that has S_8 symmetry and contains eight squares and two octagons in the hexagonal network [6]. The S_8 cage is related to the $B_{28}N_{28}$ or $B_{32}N_{32}$ (4,4) closed nanotubes in Ref. [2] and can be derived from $B_{28}N_{28}$ by eliminating a middle ring of alternating BN atoms followed by rotation by 45° . The energy differences between these isomers, particularly between the S_8 and S_4 cages are quite small (0.1eV or less) and thus based on energetics it is not apparent which isomer is most likely to be observed in the experiment. Clearly more theoretical calculations or further experimental characterization is necessary. For this purpose we have carried out density functional [8] calculations on the three candidate structures of the $B_{24}N_{24}$ clusters. We predict the infra-red (IR) and Raman spectra for the three isomers which may aid the experimentalists in identifying the structure of $B_{24}N_{24}$. Along with these spectra we also report the ionization potential, and the static dipole polarizability of the three cages. Our calculations are carried out at the all electron level by the NRLMOL code [9,10,11], using large polarized Gaussian basis sets [12] optimized for these density functional calculations, and using the Perdew-Burke-Ernzerhof generalized gradient approximation (PBE-GGA) [13].

The energetics and the electronic properties of optimized structures are summarized in Table 1. The calculations predict the S_8 cage as the lowest energy structure. The S_4 isomer is within 0.03 eV while the \emptyset cage is 2.6 eV higher. This energy ordering is in accord with earlier hybrid density functional (B3LYP/6-31G*) calculations [6]. These energy differences are of same magnitude even with addition of the zero-point energy. The vibrational frequencies determined within the harmonic approximation indicate all structures to be local minima on the potential energy surface. Further, consistent with earlier prediction on the BN cages and nanotubes [14], these cages are characterized

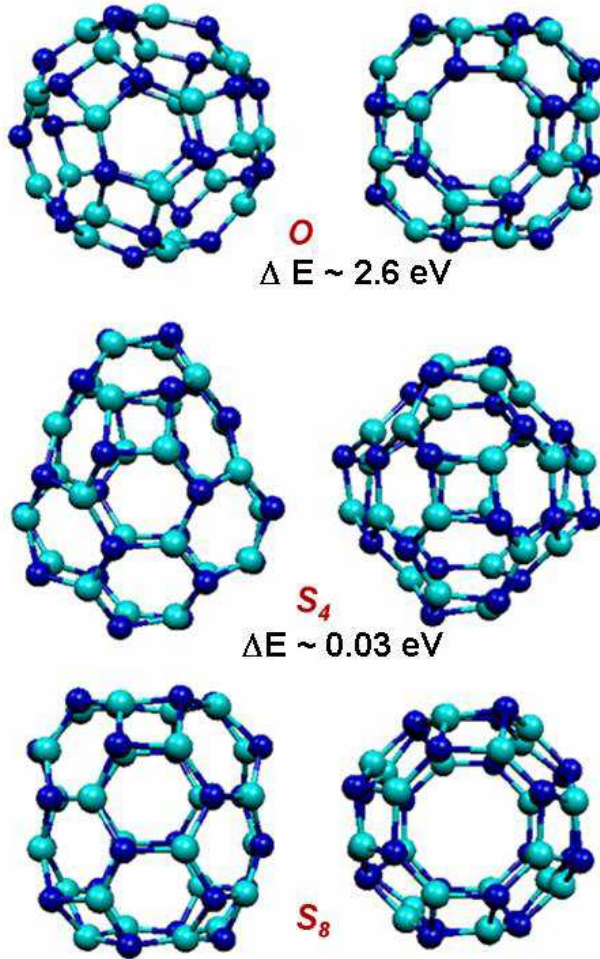


Fig. 1. (Color online) Two different views of optimized $B_{24}N_{24}$ cages. The relative energies are given with respect to S_8 total energy.

Table 1

The total electronic energy E (in Hartree), the zero point energy (ZPE), ΔE (energy relative to the energy of S_8 cage and excluding ZPE contribution) (in kJ/mol), binding energy (BE) per atom (in eV), the vertical ionization potential (VIP) (in eV), and the HOMO-LUMO gap (in eV) of the $B_{24}N_{24}$ cages. The ZPE is half the sum of vibrational frequencies.

	E	ZPE	ΔE	BE	VIP	gap
\emptyset	-1910.96994	664.49	2.6	8.27	8.4	4.7
S_4	-1911.06552	678.74	0.03	8.32	8.5	4.9
S_8	-1911.06676	675.02	0.0	8.32	8.3	4.6

by a wide energy gap of about 4.7 eV between the highest occupied molecular orbital (HOMO) and the lowest unoccupied molecular orbital (LUMO). We note that the HOMO-LUMO gaps obtained within the present PBE-GGA generally underestimate the sum of ionization potential and electron affinity.

Table 2

The static dipole polarizability (in \AA^3) of the \emptyset , S_4 , and S_8 isomers of $B_{24}N_{24}$.

	α_{xx}	α_{yy}	α_{zz}	$\bar{\alpha}$
\emptyset	53.8	53.8	53.8	53.8
S_4	49.3	49.3	55.6	51.4
S_8	50.7	50.7	55.4	52.3

Table 3

The IR active frequencies of $B_{24}N_{24}$ cages. The quantity inside the bracket is the intensity ($\text{Debye}^2/\text{amu}/\text{\AA}^2$) the respective absorption. Only IR active modes with intensity greater than 3 ($\text{Debye}^2/\text{amu}/\text{\AA}^2$) are given.

	Symmetry	Frequency (cm^{-1})
\emptyset	T_1	759 (7), 1471 (83)
S_4	B	1368 (7), 1423 (47), 1448 (34)
	E	1353 (7), 1399 (26), 1442 (30)
S_8	B	1432 (87)
	E_1	767 (7), 1406 (27), 1461 (45).

The vertical ionization potential (VIP) is calculated from the the differences in total energy of the self-consistent solution of the cluster and its singly charged positive ion, at the optimal ionic configuration of the neutral cluster. The calculated VIP are also given in Table 1. We note that the VIP reported for the $\emptyset B_{24}N_{24}$ cage in Ref. [2] should be 8.64 eV instead of incorrectly reported value of 6.66 eV. The vertical electron affinity calculations can be performed in similar fashion. We find that the additional electron is weakly bound (despite relatively large basis set used in the calculation its eigenvalue turns out to be positive although the total energy is lowered with respect to neutral cluster).

The static dipole polarizability is an important physical quantity that characterizes the electric response of the clusters to applied uniform electric field. It is calculated from the so called *finite field* method in which the self-consistent problem is solved for the usual Hamiltonian augmented with the field term $\vec{E} \cdot \vec{r}$. The polarizability tensor is built from the self-consistent solutions performed for various values of electric field E along different directions. The nuclei are assumed to be frozen. The calculated values are shown in Table 2. The mean polarizability of the three isomers is of similar magnitude with the \emptyset cage being slightly more polarizable. The structural differences of the isomers are reflected in the anisotropy of the polarizability. Unlike the perfectly round \emptyset cage, the isomers S_8 and S_4 have nonzero anisotropy.

The calculated IR spectra are presented in Fig. 2. The frequencies and their symmetries of IR active modes are listed in Table 3. The IR absorption in-

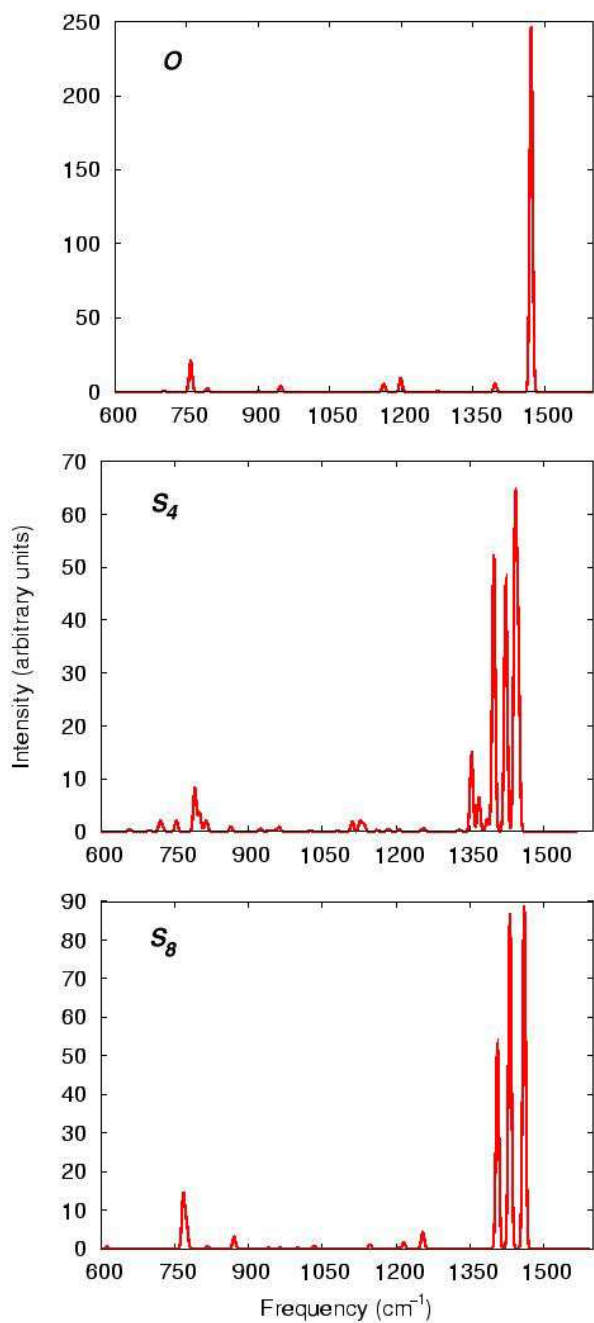


Fig. 2. The infra-red spectra of the three cage structures of the $B_{24}N_{24}$.

tensities are broadened by 6 cm^{-1} to mimic experimental uncertainties. The IR spectra of the three isomers have different structure. The high symmetry of the round O cage results in its IR spectrum with four peaks. It shows a strong absorption at 1471 cm^{-1} and a weak absorption at 759 cm^{-1} . Other peaks around 950 cm^{-1} and 500 cm^{-1} have relative intensity less than 2%.

Table 4

The Raman active frequencies of $B_{24}N_{24}$ cages. (Frequencies with very weak absorption are not presented).

	Symmetry	Frequency (cm^{-1})
\emptyset	T_2	150
	A_1	428, 780, 790, 901
	E	131, 910
S_4	A	192, 215, 472, 760, 794, 820
	E	236
S_8	A	262, 469, 798
	E_2	158, 247

The strong absorption mode at 1471 cm^{-1} is three fold degenerate and corresponds to stretching and a compression of the alternate bond in the octagon. An earlier IR calculation [7] on the $\emptyset B_{24}N_{24}$ cage that used semi-empirical modified neglect of diatomic overlap (MNDO) method reports three very different IR active modes at 1356 , 1336 , and 772 cm^{-1} . The IR spectra of S_4 can be broadly classified into two categories of bands in the frequency range $1353\text{-}1448 \text{ cm}^{-1}$. The first set consists of small peaks around 1350 cm^{-1} while the second set shows three peaks at 1399 , 1423 , and at $1442\text{-}1448 \text{ cm}^{-1}$. In the experiment, the later set of peaks may show up as a broad band beginning with a shoulder around 1350 cm^{-1} . The IR spectra of the S_8 structure exhibits three conspicuous peaks at 1407 , 1432 , and 1461 cm^{-1} . The strongest mode at 1432 cm^{-1} corresponds to a compression of two opposite hexagonal bonds accompanied by simultaneous stretching of remaining hexagonal bonds. The absorption at 1461 cm^{-1} is due to the compression and stretching of bonds of octagons. A small peak is also observed at lower frequency of 767 cm^{-1} . It corresponds to a vibrational mode that results in puckering of alternate atoms. The differences observed in the structure of the predicted IR spectra of the three isomers indicate the possibility of identifying the isomer by high resolution IR spectroscopy measurement. A sharp, high-frequency peak would indicate the presence of the octahedral isomer.

The Raman spectra of the three $B_{24}N_{24}$ cages are shown in Fig. 3 and the vibrational frequencies at which significant absorption occurs are presented in Table 4. The Raman spectra of three cages show an interesting feature: all three cages show an intense absorption in the $420 - 480 \text{ cm}^{-1}$ region. In all the three structures this mode is an A mode and corresponds to the breathing motion of the cages. The intensity of this peak is comparable in all the three structures. The \emptyset cage is marked by an intense double peak in the $131\text{-}150 \text{ cm}^{-1}$ region which is not seen in the other two spectra. These peaks are associated with E and T_2 modes. Thus two peaks below 160 cm^{-1} and another one at

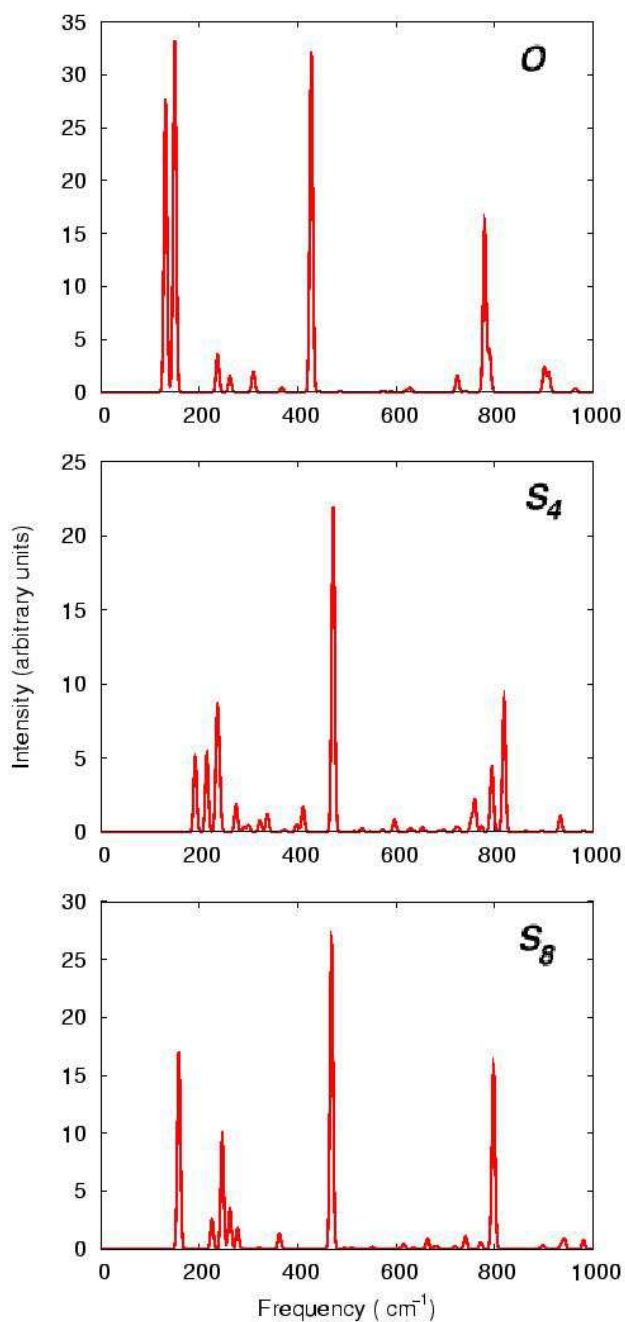


Fig. 3. The Raman spectra of the three cage structures of the $B_{24}N_{24}$.

around 430 cm^{-1} , all with similar intensity will signify a \emptyset structure. On the other hand, the S_4 structure will show three low Raman peaks in the region 190 - 230 cm^{-1} and three others around 800 cm^{-1} . In experiment, they may appear as broad peaks with roughly half the intensity of the most intense peak at 430 cm^{-1} . The \emptyset structure also shows a weak absorption around 800

cm^{-1} . The S_8 structure has a low frequency peak around 158 cm^{-1} which is about half as intense as the peak at 472 cm^{-1} , and a similar one at 798 cm^{-1} . The peak at 158 cm^{-1} due to a doubly degenerate E mode while the one at 798 cm^{-1} has A symmetry. Further it will show a broad band at 230 cm^{-1} which will be missing in the two other structures. These differences in the Raman spectra of the \emptyset , S_4 , and S_8 cages may help in identifying them in the experimental spectra.

To summarize, three candidate structures for the ground state geometry of the $B_{24}N_{24}$ are considered. These are, the octahedral structure proposed by the experimentalists, the S_4 cage that satisfy the isolated square rule, and the S_8 symmetric tubule containing two octahedrons and eight squares. The harmonic frequency analysis indicate all structures to be vibrationally stable. The S_8 tubule and S_4 are energetically nearly degenerate and are favored over the \emptyset cage on the basis of energetics. All the three clusters have wide HOMO-LUMO gap and high ionization potential. The infra-red and Raman spectra show notable differences and therefore point to possible identification of the structure by the IR or Raman spectroscopy. The IR spectra perhaps, as in the case of C_{60} [15,16], could guide methods for optimizing the production of the round cluster.

The Office of Naval Research, directly and through the Naval Research Laboratory, and the Department of Defense's High Performance Computing Modernization Program, through the Common High Performance Computing Software Support Initiative Project MBD-5, supported this work.

References

- [1] T. Oku, A. Nishiwaki, I. Narita, M. Gonda, Chem. Phys. Lett. **380** (2003) 620.
- [2] R. R. Zope, B. I. Dunlap, Chem. Phys. Lett. **386** (2004) 403.
- [3] J. W. Mintmire, B. I. Dunlap, C. T. White, Phys. Rev. Lett. **68** (1992) 631.
- [4] H.-Y. Zhu, T. G. Schmalz, D. J. Klein, Int. J. Quantum Chem. **63** (1997) 393.
- [5] M.-L. Sun, Z. Slanina, S.-L. Lee, Chem. Phys. Lett. **233** (1995) 279.
- [6] H. Wu, H. Jiao, Chem. Phys. Lett. **386** (2004) 369.
- [7] V. V. Pokropivny, V. V. Skorokhod, G. S. Oleinik, A. V. Kurdyumov, T. S. Bartnitskaya, A. V. Pokropivny, A. G. Sisonyuk, D. M. Sheichenko, J. Solid State Chem. **154** (2000) 214.
- [8] W. Kohn, L. J. Sham, Phys. Rev. **140** (1965) A1133.
- [9] M. R. Pederson, K. A. Jackson, Phys. Rev. B. **41**, 7453 (1990).

- [10] K. A. Jackson, M. R. Pederson, Phys. Rev. B. **42**, 3276 (1990).
- [11] M. R. Pederson, K. A. Jackson, Phys. Rev. B. **43**, 7312 (1991).
- [12] D. V. Porezag, M. R. Pederson, Phys. Rev. A **60**, 2840 (1999).
- [13] J. P. Perdew, K. Burke, M. Ernzerhof, Phys. Rev. Lett. **77** , 3865(1996).
- [14] X. Blase, A. De Vita, J.-C. Charlier, R. Car, Phys. Rev. Lett. **80** (1998) 1666.
- [15] Z. C. Wu, D. A. Jelski, and T. F. George, Chem. Phys. Lett. **137**, (1987) 291.
- [16] W. Krättschmer, K. Fostiropoulous, D. R. Huffman, Chem. Phys. Lett. **170**, (1990) 167.